Polymer 49 (2008) 2745–2754

Contents lists available at ScienceDirect

Polymer

journal homepage: www.elsevier.com/locate/polymer

A highly active novel β-nucleating agent for isotactic polypropylene

Shicheng Zhao [a], Zhi Cai [b], Zhong Xin [a,*]

[a] State-Key Laboratory of Chemical Engineering, East China University of Science and Technology, Shanghai 200237, People's Republic of China
[b] China petroleum and Chemical Corporation, Jiujiang, Jiangxi Province, People's Republic of China

ARTICLE INFO

Article history:
Received 12 November 2007
Received in revised form 26 March 2008
Accepted 2 April 2008
Available online 12 April 2008

Keywords:
Polypropylene
Nucleating agent
Crystallization behavior

ABSTRACT

A highly active novel β-nucleating agent for isotactic polypropylene (iPP), cadmium bicyclo[2.2.1]hept-5-ene-2,3-dicarboxylate (BCHE30), was found and its effects on the mechanical properties, the content of β-crystal, and crystallization behavior of iPP were investigated, respectively. The results show that the impact strength and crystallization peak temperature of nucleated iPP are greatly increased, while the spherulite size of nucleated iPP is dramatically decreased than that of pure iPP. The content of β-form of nucleated iPP (k_β value) can reach 87% with 0.1 wt% BCHE30. The Caze method was used to study the non-isothermal crystallization kinetics of nucleated iPP and the crystallization active energy was achieved by Kissinger method.

1. Introduction

Recently, β-nucleated isotactic polypropylene (β-iPP) has received considerable interests due to its excellent thermal and mechanical performance [1–18]. The toughness and thermal deformation temperature of β-iPP are much higher than that of the α-iPP, which is very important from the viewpoint of industrial application. However, due to its lower stability in comparison with the α-modification, the β-modification occurs sporadically and can only be formed under some critical conditions such as quenching the melt to a certain temperature range [4,5], directional crystallization in a thermal gradient field [6,7], shearing or elongation of the melt during crystallization [8], vibration-induced crystallization [9,10], or using β-nucleating agents [1,11–18].

Of these methods the addition of β-nucleating agents is most effective to obtain a high level of the β-phase. Until now, only three classifications of compounds have been mainly used as β-form nucleating agents: the first one is organic pigment [11–13], such as γ-quinacridone (Dye Permanent Red E3B), Indigosol Grey/IBL, Indigosol Golden Yellow IGK, and Cibantine Blue 2B; the second one includes a minority of aromatic amide compounds [1,14,15], such as *N,N′*-dicyclohexylterephthalamide and *N,N′*-dicyclohexyl-2,6-naphthalene dicarboxamide (trade name NJStar NU-100); the third classification comprises certain group IIA metal salts or their mixtures with some specific dicarboxylic acids [16–18], such as calcium salt of imido acids and compounds of calcium stearate and pimelic acid. However, so far, there are no literatures about IIB salts of alicyclic dicarboxylate acid acting as β-nucleating agents. In our study, we found that cadmium bicyclo[2.2.1]hept-5-ene-2,3-dicarboxylate (BCHE30) was an effective β-nucleating agent for iPP.

In this paper, the effects of the novel β-nucleating agent BCHE30 on the mechanical properties, the content of β-crystal, crystallization peak temperature (T_{cp}) and the crystal morphology of iPP were investigated. In addition, the non-isothermal crystallization kinetics of both pure iPP and iPP/BCHE30 were investigated by using the Caze method [19]. The crystallization activation energy was evaluated by Kissinger's method [20].

2. Experimental

2.1. Materials

The isotactic polypropylene (iPP) (trade name F401, $M_w = 307\,000$, $M_n = 81\,000$, MWD = 3.8) used in this study was kindly provided by Yangzi Petrochemical Corporation (China). The material has a melt flow index (MFI) of 3.4 g/10 min. The β-nucleating agent is cadmium bicyclo[2.2.1]hept-5-ene-2,3-dicarboxylate (BCHE30), which is synthesized according to the patent [21]. The results of carbon and hydrogen elemental analyses and infrared spectroscopy of BCHE30 indicate that its simple molecular structure corresponds to $CrOOCC_7H_8COO$. According to DSC and TG results under nitrogen atmosphere, BCHE30 has excellent thermal stability.

2.2. Sample preparation

The nucleating agent BCHE30 and the iPP powders were dry-blended by high-speed mixer for 5 min. Then the mixture was

* Corresponding author. Tel.: +86 21 64252972; fax: +86 21 64240862.
E-mail address: xzh@ecust.edu.cn (Z. Xin).

0032-3861/$ – see front matter © 2008 Elsevier Ltd. All rights reserved.
doi:10.1016/j.polymer.2008.04.012

extruded by a twin-screw extruder (SJSH-30, Nanjing Rubber and Plastics Machinery Plant Co., Ltd.) through a strand die and pelletized. The pellets were molded into standard test specimens by an injection-molding machine (CJ-80E, Guangdong Zhende Plastics Machinery Plant Co., Ltd.). The concentrations of the nucleating agent were 0.025, 0.05, 0.075, 0.1, 0.2, 0.4, 0.6 and 1.0 wt% and the samples were denoted as PP1, PP2, PP3, PP4, PP5, PP6, PP7 and PP8, respectively. The pure iPP sample was designated as PP0, which was prepared by the same method for comparison.

2.3. Mechanical properties

The mechanical properties were measured according to ASTM test methods, such as D-638 for the tensile strength and D-790 for the flexural modulus, using a universal testing machine (Shanghai D & G Measure Instrument Co., Ltd). The Izod impact strength was tested on the basis of D-256, using an impact tester (Chengde Precision Tester Co., Ltd).

2.4. Differential scanning calorimetry (DSC)

DSC (Diamond, Perkin–Elmer) was carried out to measure the β-crystal content, study the crystallization peak temperature and analyze the non-isothermal crystallization kinetics. Temperature was calibrated before the measurements by using Indium as a standard medium.

β-Fraction (β_c) was estimated from DSC by the following expression [22]:

$$\beta_c = (1-\lambda)_\beta / \left[(1-\lambda)_\beta + (1-\lambda)_\alpha\right]$$

The degree of crystallinity $(1-\lambda)$ associated with each phase can be calculated from the ratio $\Delta H_a/\Delta H_u$, where ΔH_a and ΔH_u are the apparent and completely crystalline heats of fusion, respectively. The values 177.0 and 168.5 J g^{-1} were used for the ΔH_u for 100% crystalline α-iPP and 100% crystalline β-iPP, respectively [23].

The crystallization peak temperatures (T_{cp}) was determined from the crystallization curves. Measurements were performed with the samples of 3–5 mg at a standard heating and cooling rate of 10 K/min under nitrogen starting from 323 to 473 K, and the samples were held at 473 K for 5 min to erase the thermal and mechanical history.

Non-isothermal crystallization experiments were carried out by cooling samples (PP5) from 473 to 323 K using different cooling rates. The exotherms were recorded at the cooling rates of 5, 10, 20, 30 and 40 K/min, respectively.

2.5. Polarized optical microscopy (POM)

The morphology studies of pure iPP and nucleated iPP were performed with the aid of an Olympus BX51 (Japan) polarized optical microscopy attached with a DP70 digital camera, and a THMS600 hot-stage. The extruded samples were placed between two microscopy slides, melted and pressed at 473 K for 5 min to erase any trace of crystal, and then rapidly cooled to a predetermined crystallization temperature. The samples were kept isothermal until the crystallization process was completed, and meanwhile, photographs were automatically taken.

2.6. Wide-angle X-ray scattering (WAXD)

Wide-angle X-ray scattering (WAXD) patterns were recorded in transmission with a Rigaku D/max-2550VB/PC apparatus. The wavelength of Cu Kα was $\lambda = 1.54$ Å and spectra were recorded in the 2θ range of 5–35° (8°/min). The content of the β-crystal modification was determined according to standard procedures described in the literature [24], employing the relation:

$$k_\beta = \frac{H_\beta(300)}{H_\beta(300) + H_\alpha(110) + H_\alpha(040) + H_\alpha(130)}$$

where k_β denotes the relative content of β-crystal form (WAXD), $H_\alpha(110)$, $H_\alpha(040)$ and $H_\alpha(130)$ are the intensities of the strongest peaks of α-form attributed to the (110), (040) and (130) planes of monoclinic cell, respectively, while $H_\beta(300)$ is the intensity of the strongest (110) diffraction peak of the trigonal β-form.

2.7. Theory of non-isothermal crystallization

The Avrami equation [25,26] is widely used to describe the polymer isothermal crystallization.

$$X_t = 1 - \exp(-Z(T)t^n) \tag{1}$$

where X_t is the relative crystallinity at time t, n is a constant whose value depends on the mechanism of nucleation and on the form of crystal growth, and $Z(T)$ is a constant containing the nucleation and growth parameters.

The Avrami equation has been extended by Ozawa [27] to develop a simple method to study the non-isothermal experiment. The general form of Ozawa theory is written as follows:

$$X_v(T) = 1 - \exp(-K_T/\phi^m) \tag{2}$$

where K_T is the cooling crystallization function, Φ is the cooling rate, and m is the Ozawa exponent that depends on the dimension of the crystal growth. But there is a main hypothesis in Ozawa method that n is independent of temperature and only a limited number of X_v data are available for the foregoing analysis, as the onset of crystallization varies considerably with the cooling rate.

Caze et al. [19] put forward a new method to modify Ozawa equation. They have assumed an exponential increase of K_T with T upon cooling. On the basis, the temperature at the peak and the two inflexion points of the exotherm with skew Gaussian shape are linearly related to ln Φ in order to estimate the exponent n.

On the basis of the findings on the crystallization behavior of poly(ethylene terephthalate) and PP, Kim et al. proposed [28]

$$\ln K_T = a(T - T_1) \tag{3}$$

where a and T_1 are empirical constants. If the extreme point of the pertinent $\partial X_v(T)/\partial T$ curve occurs at $T = T_q$ (crystallization peak temperature), i.e. $(\partial^2 X_v(T)/\partial T^2)T_q = 0$, we have:

$$K_T(T_q) = \phi^n \tag{4}$$

Combining Eqs. (2)–(4) yields:

$$\ln[-\ln(1 - X_v(T))] = a(T - T_q) \tag{5}$$

Hence, a linear plot of $\ln[-\ln(1 - X_v(T))]$ against T would result in the constant a and the product $-aT_q$ from the gradient and intercept, respectively. At $T = T_q$ obtained from the foregoing algorithm, Eqs. (4) and (5) lead to:

$$T_q = n \ln \phi / a + T_1 \tag{6}$$

As such, parameter n can be obtained from the linear plot of T_q against ln Φ/a in accordance with Eq. (6).

3. Results and discussion

3.1. Mechanical behavior

From the viewpoint of industrial application, it is necessary to investigate the effects of nucleating agent on mechanical

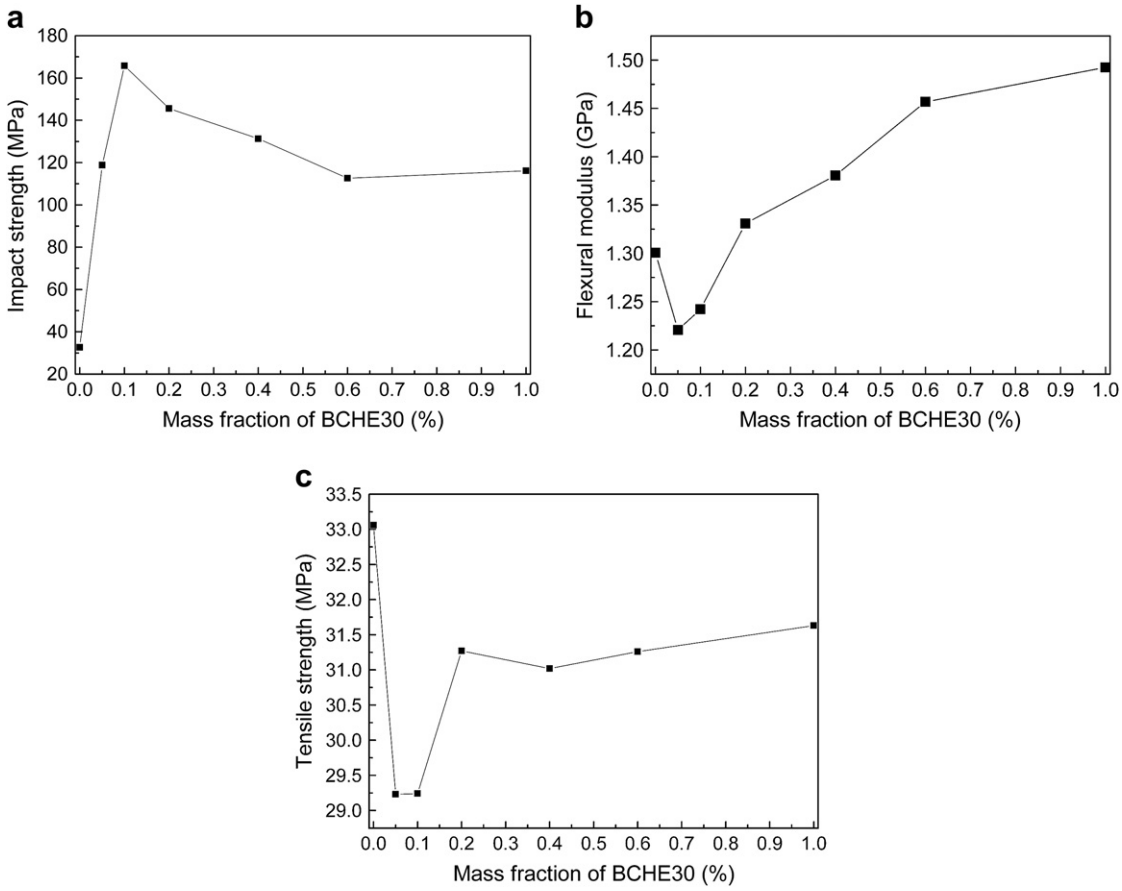

Fig. 1. The influence of mass fraction of β-nucleating agent on (a) impact strength, (b) flexural modulus and (c) tensile strength of iPP.

properties. The effects of the novel nucleating agent BCHE30 on mechanical properties of iPP are shown in Fig. 1. The impact strength increases rapidly when BCHE30 is less than 0.1 wt%, and then slightly decreases until constant with the further increase of BCHE30. When the content of BCHE30 is 0.1–0.2 wt%, the impact strength of nucleated iPP is improved about 4 times compared with that of pure iPP, indicating that BCHE30 is an effective β-nucleating agent. In Fig. 1b and c, the tensile strength and flexural modulus of nucleated iPP decrease rapidly until the concentration of BCHE30 reaches about 0.1 wt%, and then increase with the further increasing concentration, which shows a reverse tendency with that of impact strength. It can be seen that the flexural modulus of nucleated iPP is higher than that of pure iPP while the tensile strength of nucleated iPP is comparable with that of pure iPP when the nucleating agent content is about 0.2 wt%. Therefore, the 0.2 wt% seems to be an optimum addition content for BCHE30 in the industry application of iPP.

3.2. *Effect of the nucleating agent on the content of β-crystals of iPP*

For the quantification of β-phase content in isothermally crystallized iPP samples, wide-angle X-ray diffraction (WAXD) was used. Fig. 2 illustrates the WAXD patterns of PP0 and PP2 crystallized at 132 °C under quiescent condition. In this profile, (110) at $2\theta = 14.1°$, (040) at 16.9°, (130) at 18.5° are the principal reflections of the α-crystals of iPP while (300) at about 16° is the principle reflection of the β-crystals. They are considered as the marker peaks for α- and β-crystal, respectively. It shows that α-crystals exist in PP0. There is a very tiny peak around 16° which belongs to the (300) reflection of β-crystals, indicating that few β-crystals exists in PP0. Comparing with that of PP0, an obvious difference can be seen in the pattern of PP2. In this pattern, the (300) reflection of β-crystals is clearly seen at 2θ about 16°, and its intensity is greater than that of α-crystals. The k_β value of PP2 reaches 87%, which indicates that BCHE30 is an effective β-nucleating agent for iPP even at a low working concentration of 0.05 wt%.

The WAXD patterns of nucleated iPP with different contents of BCHE30 crystallized at 132 °C under static state are shown in Fig. 3.

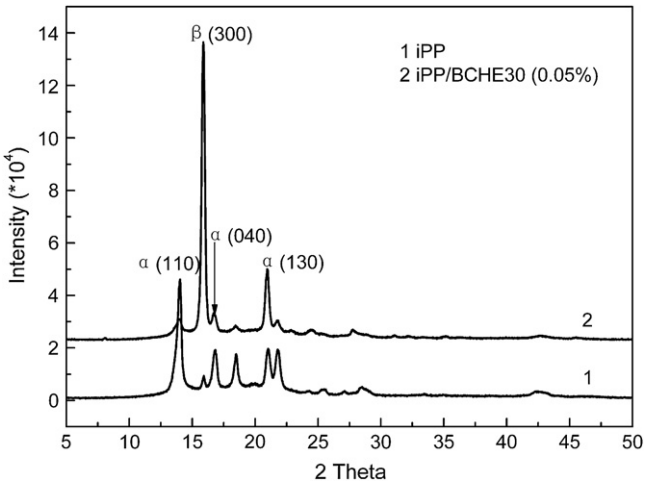

Fig. 2. WAXD patterns of sample PP0 (neat iPP) and PP2 (with 0.05% additives) crystallized at 132 °C under quiescent condition.

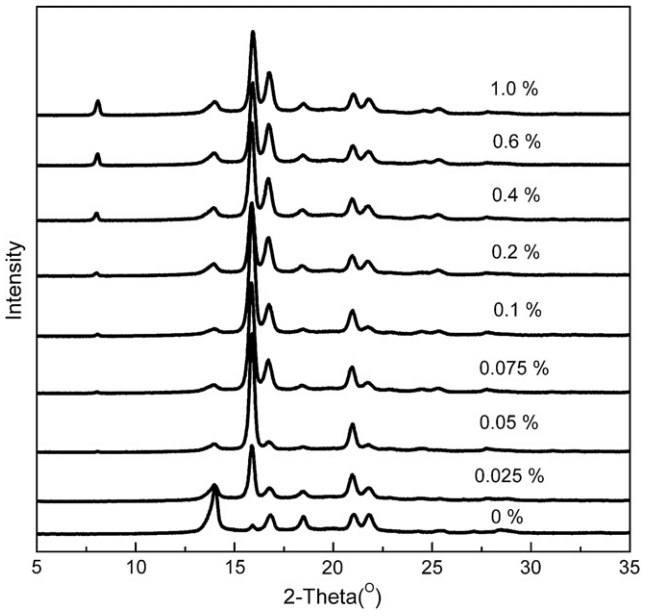

Fig. 3. WAXD patterns of sample PP0 (pure iPP) and nucleated iPP with different BCHE30 contents crystallized at 132 °C under quiescent condition.

k_β values as a function of the content of the β-nucleating agents are reported in Fig. 5. The calculation results show that the k_β value increases with the presence of BCHE30, reaches a maximum value (87%) when BCHE30 percentage is 0.05 wt%, and then decreases until constant with a further increase of BCHE30 percentage. The above results indicate that BCHE30 is an effective β-nucleating agent even at a low working concentration for iPP. However, BCHE30 is not a completely selective β-nucleating agent, as the related samples always contain both α- and β-modification of iPP. The changing trend of k_β values is basically consistent with that of the impact strength for iPP/BCHE30, which indicates that the improvement of impact strength of iPP is most likely from the increased content of β-crystal form.

For comparison, DSC was used to characterize the content of β-crystals (X_β) of the same samples with the WAXD. The DSC patterns of iPP with different contents of BCHE30 are shown in Fig. 4. The melting peak at low temperature is attributed to the β-crystals and that at high temperature belongs to the α-crystals. The relative area of β-crystals' melting peak greatly increases when the content of BCHE30 is lower than 0.05%, then gradually decreases with the further increase of nucleators and keeps constant at higher concentrations. The trend is same with that of WAXD. It is interesting that the melting peak of β-crystals shifts to high temperature until the concentration of nucleator reaches 0.05 wt% and then shifts to low temperature; while the melting peak of α-crystals shifts to high temperature with the increasing content of BCHE30. Lower melting peak temperature indicates the structural instability of β-phase. The results can be interpreted by dual nucleating activity of BCHE30, which will be discussed in detail in the subsequent section of crystallization behavior.

The dependence of k_β value (WAXD) and β_c (DSC) on the content of nucleating agent is illustrated in Fig. 5. Comparing the two curves, the trends of WAXD and DSC are similar. However, the k_β value is 5–15% higher than β_c. One reason is that the exact determination of the β-content is difficult using DSC because the melting peaks of the α- and β-modification overlap each other. Another reason is the exiting of βα-recrystallization of β-crystals during the melting. Therefore, the WAXD is more accurate than DSC to characterize the content of β-crystals of iPP.

Generally, the increase of concentration of the nucleating agents helps to increase the proportion of β-crystals. However, it can be seen from Fig. 5 that the k_β values of iPP with BCHE30 do not increase linearly with the increase of nucleator percentage, but reach a maximum value when BCHE30 percentage is about 0.05 wt%. That is, there exists a critical nucleation concentration. The dependence of the k_β values on the concentration of nucleating agents had been investigated by several researchers, and the similar trend was observed [29,30]. Su et al. [29] thought that the result attributed to the change of dispersibility of β-nucleating agents in iPP matrix, which had been confirmed by POM in their article. The similar phenomenon was found in our study. Fig. 6 shows the optical microphotographs of morphology of BCHE30 at the concentration of 0, 0.1, 0.2 and 0.6 wt% in the melt. All the optical microphotographs in Fig. 6 were taken by POM without cross-polarized light, and the morphology of BCHE30 in the iPP melt can be clearly observed. In Fig. 6a, no nucleating agents are observed for pure iPP. When BCHE30 proportion reaches 0.1 wt% (Fig. 6b), it disperses uniformly in the iPP matrix. With the further increasing of BCHE30, it begins to agglomerate, which can be seen from Fig. 6c and d. According to Su's investigation [29], the agglomeration of nucleating agent

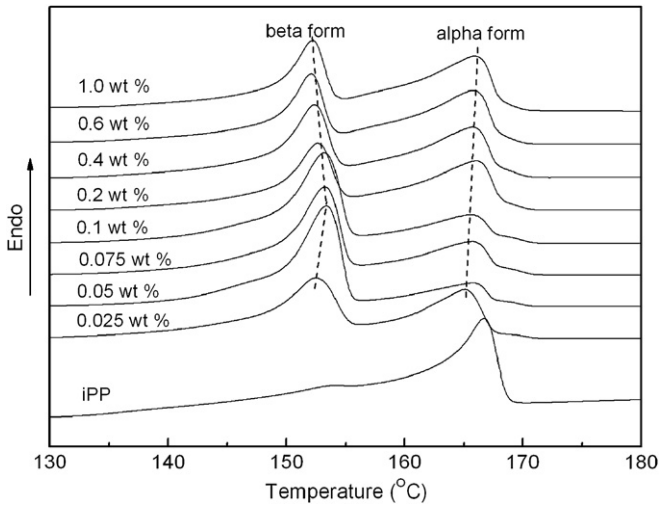

Fig. 4. The melting thermographs of iPP samples with different contents of BCHE30 isothermally crystallized at 132 °C under quiescent condition.

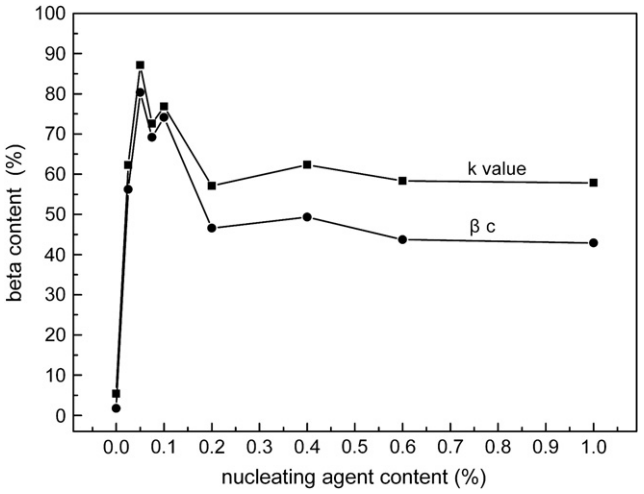

Fig. 5. k_β value and β_c as a function of BCHE30 content.

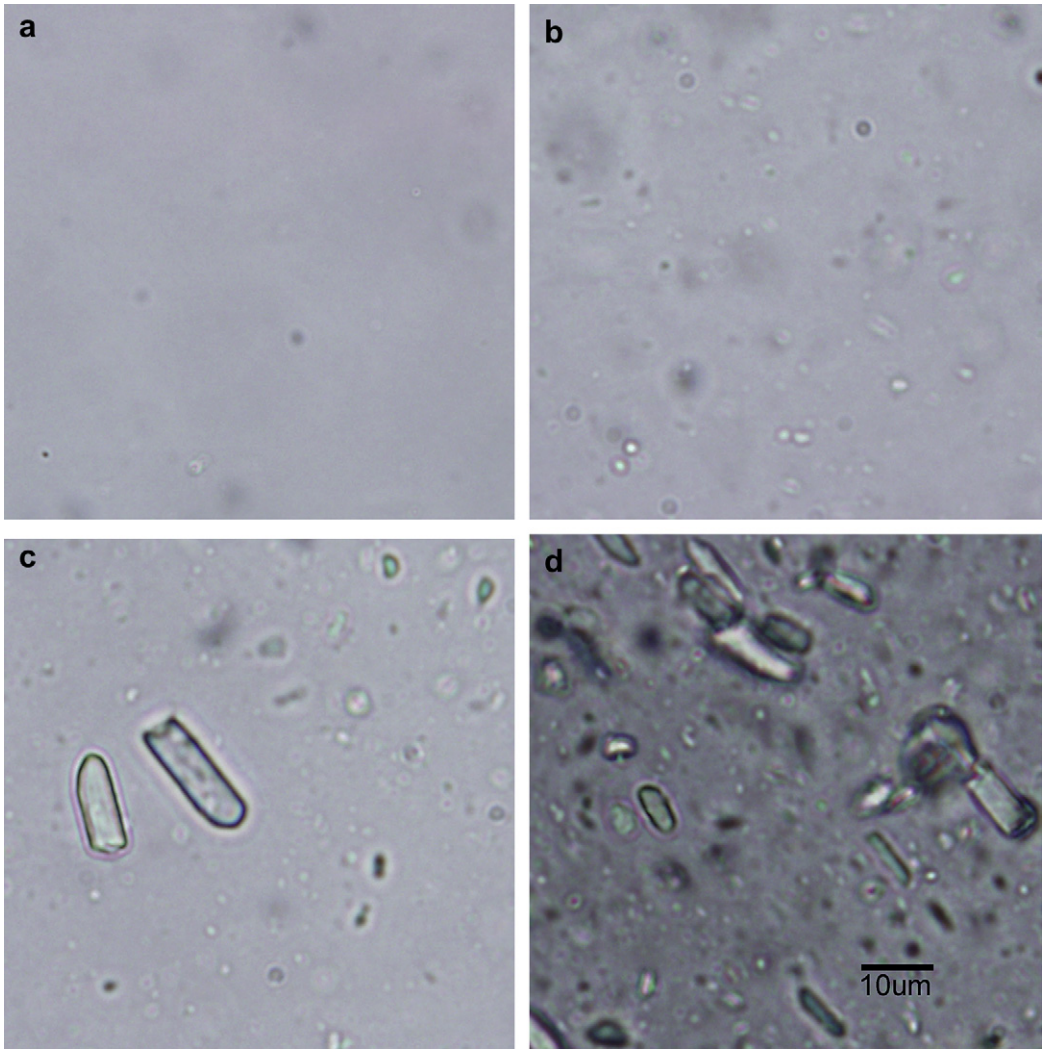

Fig. 6. Polarized light microphotographs of morphology of BCHE30 at the concentration of (a) 0, (b) 0.1, (c) 0.2 and (d) 0.6 wt% in iPP melt.

would result in the loss of β-nucleating efficiency. Therefore, in our study, the changing of k_β values can be related to the dispersibility of nucleating agents. Varga [30] proposed that the effect of nucleating agent content on the k_β values resulted from the solubility and nucleating duality of nucleating agent. In our study, the solubility of BCHE30 is not found but the nucleating duality is obvious. The mechanism that k_β value is affected by nucleating duality of BCHE30 will be discussed in detail in Section 3.3. In fact, the dispersibility and nucleating duality of nucleating agent may work simultaneously during crystallization.

3.3. Crystallization behavior

In order to check the effect of the nucleating agent on crystallization behavior, the crystallization curves of iPP with different BCHE30 contents are plotted in Fig. 7. For the pure iPP (PP0), T_{cp} is around 118 °C. However, the incorporation of only 0.075 wt% of the nucleating agent in the polymer produces a marked shift of the crystallization peak toward higher temperature ($T_{cp} = 128$ °C). T_{cp} of iPP shifts to higher temperature with the increasing of BCHE30 content. Fig. 8 shows a plot of T_{cp} as a function of BCHE30 content. It can be seen that the increase of T_{cp} is very strong when the content of BCHE30 is lower than 0.2 wt%, while that is weak when the content of BCHE30 is higher than 0.2 wt%. It indicates that 0.2 wt% is the saturated concentration and more nucleating agent is less effective in increasing the crystallization peak temperature further. Compared with pure iPP, T_{cp} of iPP with 0.2 wt% BCHE30 is increased by 13.3 °C.

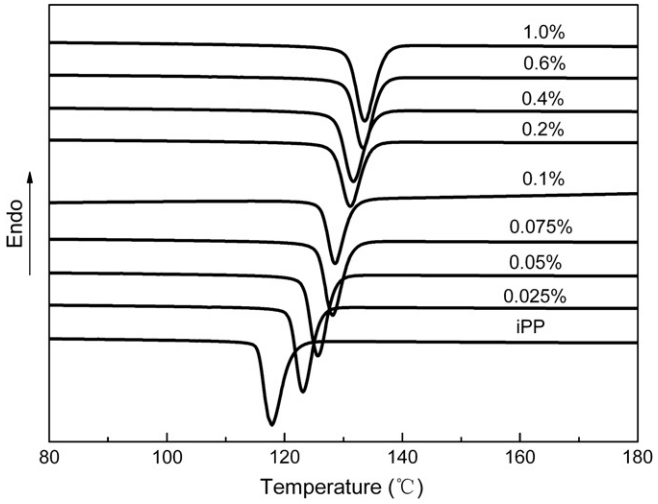

Fig. 7. Crystallization curves of pure iPP and nucleated iPP.

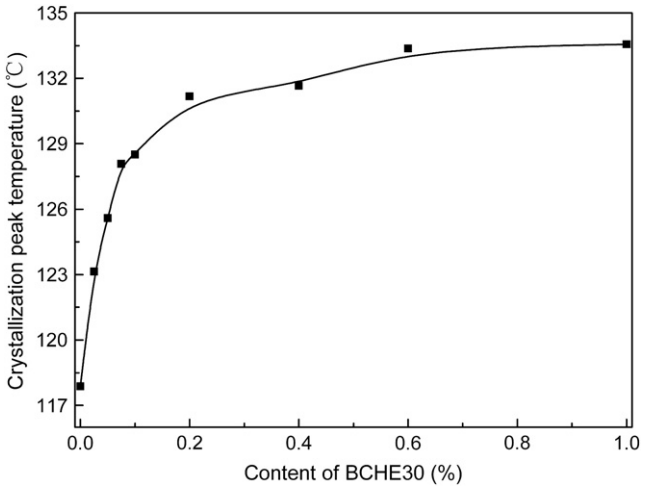

Fig. 8. Dependence of the crystallization peak temperature on the content of BCHE30.

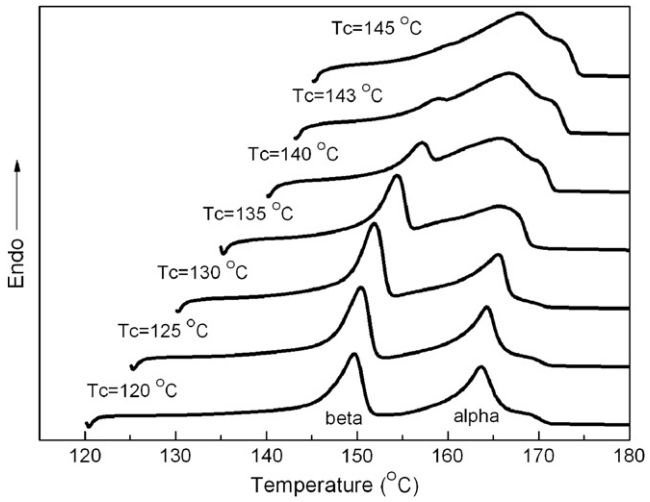

Fig. 10. The effect of crystallization temperature on the DSC melting traces of β-nucleated iPP samples ($C = 0.2$ wt%, $V_c = 100$ °C/min, $V_h = 10$ °C/min).

The isothermal crystallization of iPP and nucleated iPP was studied by DSC. The crystallization half-time ($t_{1/2}$) and melting curves of isothermally crystallized samples are shown in Figs. 9 and 10 as a function of temperature, respectively. From Fig. 9, it can be seen that $t_{1/2}$ is greatly decreased with the addition of BCHE30 and the nucleating effect is more significant with the increasing crystallization temperature. From Fig. 10, it can be seen that the relative amount of the β-phase (β_c) gradually decreases with the increasing crystallization temperature and $\beta_c \to 0$ when the crystallization temperature is higher than 140 °C. The results show that the β-nucleating ability gradually decreases while α-nucleating ability gradually increases with the increasing crystallization temperature. It is obvious that BCHE30 has dual nucleating activity and can induce both α- and β-nucleation in iPP, which may be related to nucleation mechanism of β-nucleating agent. However, the crystal structures of BCHE30 have not been established and the nucleation mechanism of BCHE30 is still unknown and needs further investigation.

Dual nucleating activity of BCHE30 can give a reasonable explanation to the effects of nucleating agent content on k_β values, impact strength and melting peak temperature of nucleated iPP. The α-nucleating ability of BCHE30 gradually increases with its increasing concentration. On the other hand, as the BCHE30 content increases, the crystallization temperature increases, which also contribute to the increase of α-nucleating ability. Considering the fact that the critical concentration of BCHE30 is low, below the critical concentration, α-nucleating activity has less effect on the k_β value and β-nucleating ability is dominant. It would result in the increase of k_β value and structural stability of β-phase with the increasing concentration of BCHE30. The α-nucleating activity cannot be neglected when the concentration of BCHE30 is higher than the critical concentration. The competition of α- and β-nucleating activity would result in the decrease of the k_β value and structural stability of β-phase, while it would lead to the increase of structural stability of α-phase with the increasing concentration of BCHE30 (Figs. 4 and 5). The decrease of k_β values results in the decrease of impact strength of nucleated iPP.

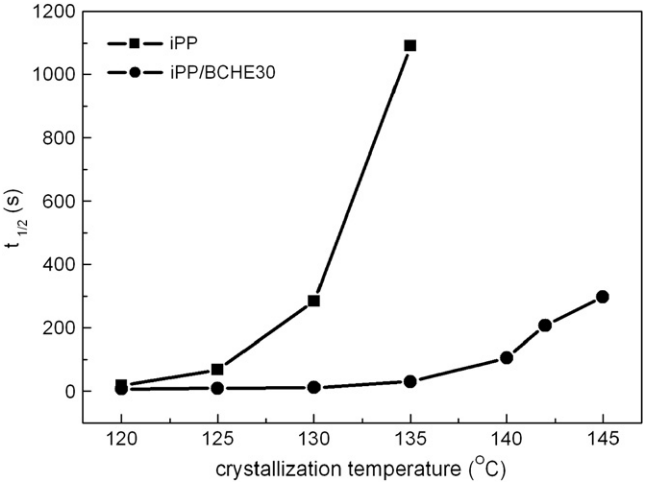

Fig. 9. The effect of crystallization temperature on the $t_{1/2}$ of iPP and β-nucleated iPP samples.

Polarized optical micrographs of pure iPP and nucleated iPP with different concentrations of BCHE30 crystallized under isothermal conditions are shown in Fig. 11. For the pure iPP (PP0), the spherulite diameter is more than 100 mm. The incorporation of BCHE30 greatly decreases the spherulite size even if its content is low. Furthermore, the spherulite size decreases greatly before the concentration of nucleating agent reaches 0.2 wt% and then decreases slightly with a further increase of BCHE30. This is in good agreement with the result of crystallization peak temperature. It is well known that the crystallization process includes the nucleation and the crystal growth. In pure iPP the formation of nuclei is difficult, thus spherulite growth is mainly a homogeneous nucleation, followed by nucleation-controlled spherulite growth. As the nucleation rate is slow and number of nucleus is few, the spherulite of iPP can become very large before it impinges another spherulite. While in nucleated iPP, a large number of nuclei would be produced because of the existence of nucleating agent. The nucleation rate is very fast and the spherulite growth in it is a heterogeneous nucleation, followed by a diffusion-controlled growth. Because of the existence of a great deal of nuclei, the spherulite cannot grow large enough to overlap, so the size of spherulites in nucleated iPP would be much smaller than those in pure iPP.

3.4. Non-isothermal crystallization kinetics

Crystallization process of semi-crystalline polymers can have a dramatic impact on the mechanical properties and hence is important to final application. Practical processes usually proceed under non-isothermal crystallization conditions. In order to search

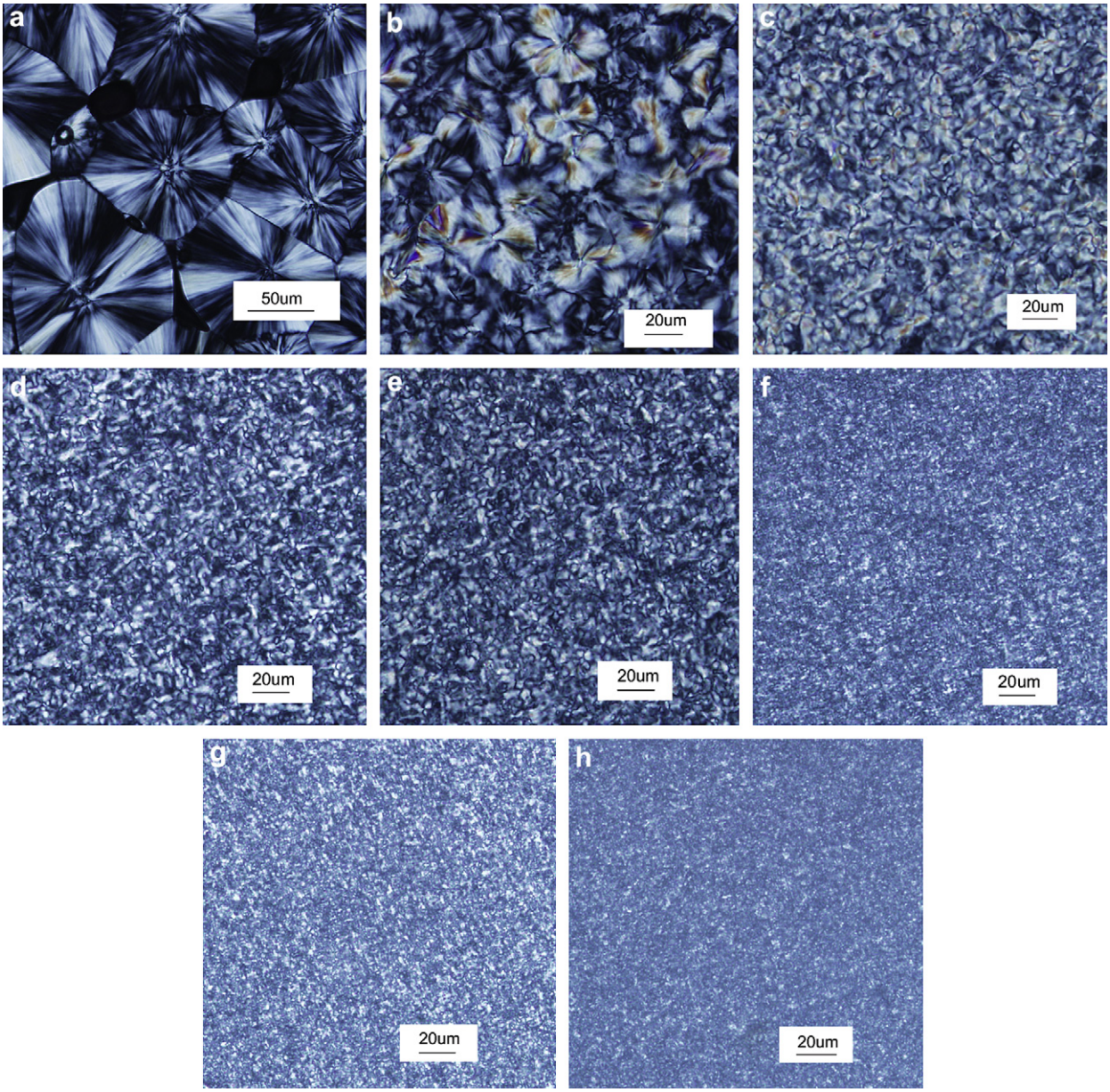

Fig. 11. Micrographs for pure iPP and nucleated iPP sample crystallized at 140 °C: (a) pure iPP, (b) 0.025, (c) 0.05, (d) 0.075, (e) 0.1, (f) 0.2, (g) 0.4, (h) 0.6 wt%.

for the optimum conditions in the industrial process and to obtain products with better properties, it is necessary to have quantitative evaluations on the non-isothermal crystallization process. The 0.2 wt% content of BCHE30 is chosen considering the fact that nucleated iPP shows better comprehensive mechanical properties at the content. The non-isothermal crystallization of iPP and nucleated iPP was carried out by DSC with cooling rates from 2.5 to 30 °C/min. The thermograms of neat iPP and nucleated iPP are plotted in Fig. 12. It is evident that the crystallization temperature is affected by the cooling rate: the higher the cooling rate, the lower the crystallization peak temperature. Furthermore, it can be recognized that, at the same cooling rates, T_{cp} of nucleated iPP is greatly increased compared with virgin iPP.

By means of integrating the partial areas under the DSC endotherm, the values of the crystalline weight fraction $X_w(T)$ can be obtained, as shown in Fig. 13.

Crystallization half-time $t_{1/2}$ can be obtained, from Fig. 13, by equation $t = (T_0 - T)/\phi$(where t is crystallization time, T_0 is the onset crystallization temperature, T is crystallization temperature at $X_w(T) = 50\%$ and Φ is cooling rate). The results are listed in Table 1. It can be seen that the addition of BCHE30 can obviously shorten $t_{1/2}$ of iPP, especially at higher cooling rate. When the cooling rate is 30 °C/min, $t_{1/2}$ of iPP/BCHE30 is 17 s while that of pure iPP is 44 s.

Now $X_w(T)$ can be converted into $X_v(T)$ by Eq. (7) [28]:

$$X_v(T) = \frac{X_w(T)\frac{\rho_a}{\rho_c}}{1 - (1 - \rho_a/\rho_c)X_w(T)} \tag{7}$$

where ρ_a and ρ_c are the bulk densities of the polymer in the amorphous and pure α- or β-crystalline states, respectively. For iPP, the density of the amorphous phase is $\rho_a = 0.852$, and those of the pure α-crystalline phase and pure β-crystalline phase are $\rho_{c\alpha} = 0.936$ [31,32] and $\rho_{c\beta} = 0.922$ [33,34], respectively. Accordingly, plots of $\ln[-\ln(1 - X_v(T))]$ vs. T can be obtained (Fig. 14) and there is a good linear relationship in the initial crystallization stage. The values of a and $-aT_q$ can be determined from the slope and

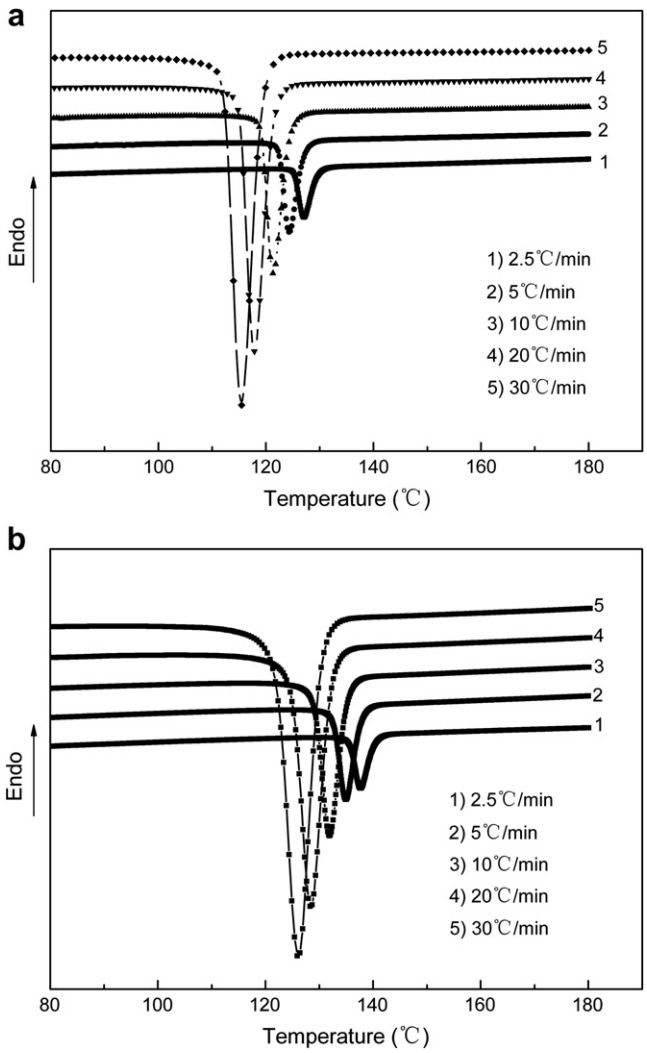

Fig. 12. DSC cooling curves of (a) iPP and (b) iPP/BCHE30 (0.2 wt%).

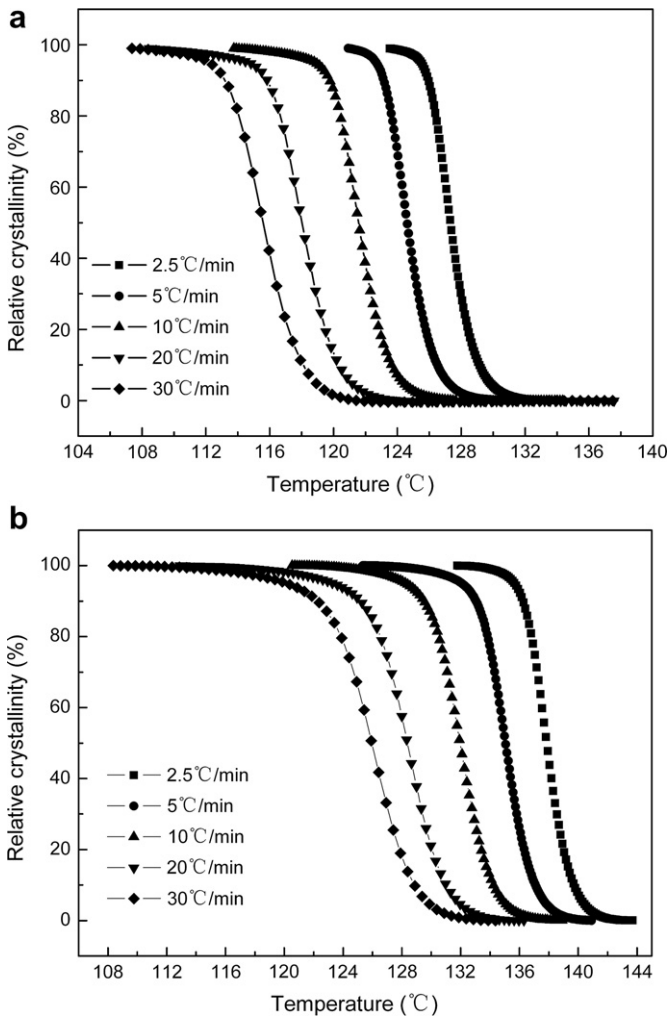

Fig. 13. Relative crystallinity of (a) virgin iPP and (b) iPP/BCHE30 (0.2 wt%) at different cooling rates.

intercept of each straight line, and the results are also listed in Table 1.

Straight lines can be obtained from plots of T_q vs. ln Φ/a under different cooling rates (Fig. 15), and Avrami exponents of iPP and nucleated iPP can be determined from the slope of each straight line. The results are also listed in Table 1. The Avrami exponent n of pure iPP is 3.86, which indicates that the spherulite growth occurs with homogeneous nucleation and three-dimension spherical growth. The Avrami exponent n for nucleated iPP is 3.22, indicating that BCHE30 acts as heterogeneous nuclei followed by three-dimension spherical growth during non-isothermal crystallization. Therefore, the type of nucleation of iPP is significantly changed in the presence of nucleating agent BCHE30 while the geometry of crystal growth of iPP does not change.

3.5. Crystallization active energy

Considering the influence of the cooling rates on the non-isothermal crystallization process, Kissinger proposed that the activation energy could be determined by calculating the variation of the crystallization peak with the cooling rate [20].

$$\mathrm{d}\ln\left(\phi/T_p^2\right)/\mathrm{d}(1/T_p) = -\Delta E/R \tag{8}$$

where Φ is the cooling rate, T_p is the crystallization peak temperature, and R is the gas constant. The crystallization activation energy (ΔE) is calculated from the slope of $\ln(\phi/T_p^2)$ vs. $1/T_p$. As shown in Fig. 16, the ΔE of pure iPP and nucleated iPP during non-isothermal crystallization is determined to 283.3 and 300.4 kJ/mol, respectively. In comparison, the ΔE of nucleated iPP is slightly higher than that of pure iPP. From the kinetic viewpoint, the activation energy could be correlated with the crystallization rate. Generally, high crystallization activation energy would hinder the crystallization and result in the decrease of crystallization rate. However, an opposite result is obtained in our study. The addition of BCHE30 increases the crystallization activation energy of iPP, but

Table 1
Non-isothermal crystallization kinetics parameters for pure iPP and nucleated iPP

Sample	Φ, °C/min	T_p,[a] °C	a	T_q,[b] °C	$t_{1/2}$, s	n
iPP	2.5	127.1	−1.09	127.0	164	3.86 ± 0.03
	5	124.4	−1.07	124.3	84	
	10	121.3	−1.00	121.2	76	
	20	117.9	−0.92	117.6	59	
	30	115.5	−0.87	115.1	44	
iPP/BCHE30	2.5	137.7	−1.16	137.6	140	3.22 ± 0.12
	5	135.0	−1.07	134.8	70	
	10	131.9	0.96	131.6	42	
	20	128.3	−0.82	128.0	25	
	30	125.9	−0.75	125.5	17	

[a] Determined from Fig. 12.
[b] Calculated from Caze method.

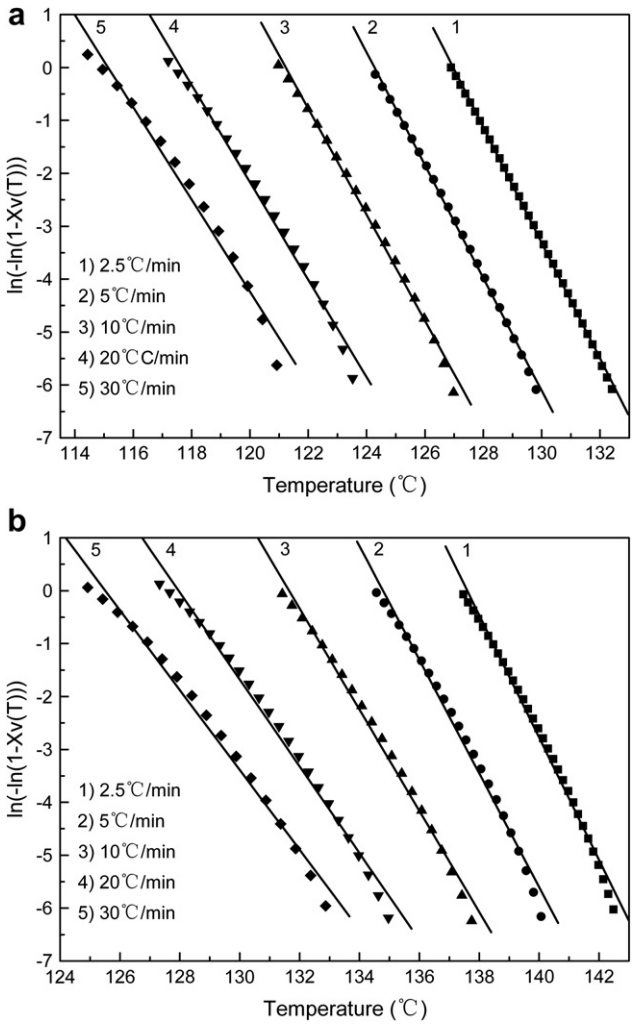

Fig. 14. Plots of $\ln[-\ln(1 - X_V(T))]$ vs. T for (a) virgin iPP and (b) iPP/BCHE30 (0.2 wt%).

it increases the crystallization rate. The similar results were reported for other nucleating agents by several researchers [35,36]. It has been considered that the effect of nucleating agent on polypropylene crystallization is twofold. On one hand, nucleating agents can serve as heterogeneous nucleating sites and favors

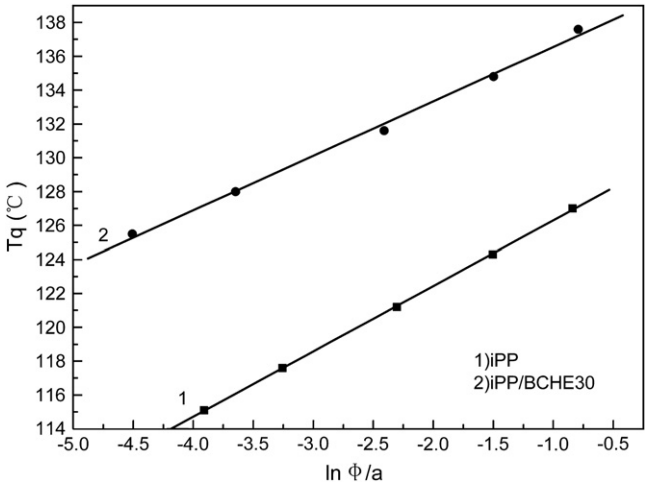

Fig. 15. Plots of T_q vs. ln Φ/a for virgin iPP and iPP/BCHE30 (0.2 wt%).

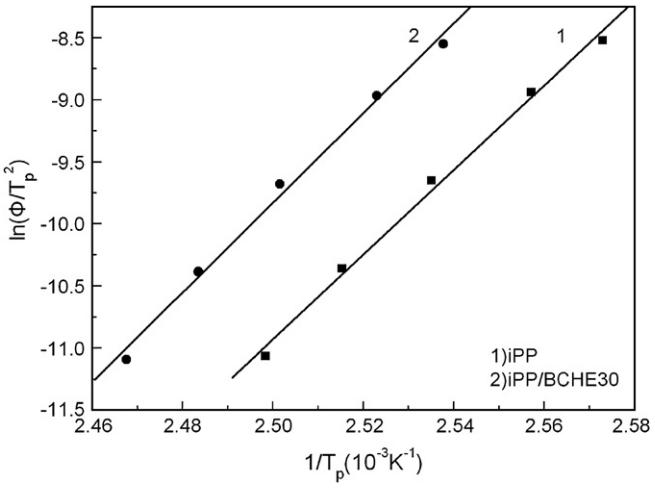

Fig. 16. Kissinger plot for calculating the non-isothermal crystallization activation energies for pure PP and iPP/BCHE30 (0.2 wt%).

crystallization growth of molecular in interface; on the other hand, nucleating agents may baffle the transfer of macromolecular segments from iPP melts to the crystal growth surface due to the weak interaction between nucleating agents and segments of iPP. The baffling effect may leads to the increase of ΔE. However, nucleation is the controlling step during crystallization and the increasing of nucleation rate results in the increase of the overall crystallization rate and crystallization temperature. The nucleating effect of BCHE30 can be found by POM (Fig. 11). The weak interaction between nucleating agents and segments of iPP can be confirmed by the increase of MFI value of iPP nucleated with BCHE30 than that of pure iPP.

4. Conclusions

In this work, the effects of the novel β-nucleating agent BCHE30 on the mechanical properties, the content of β-crystal, crystallization behavior and non-isothermal crystallization kinetics of iPP were investigated. The main conclusions are summarized as follows:

1. With the increase of BCHE30 concentration, the impact strength of iPP nucleated with BCHE30 first increases and then decreases until constant. At the concentration 0.1–0.2 wt%, the impact strength of nucleated iPP increases about 4 times than that of pure iPP. Meanwhile, the tensile strength and flexural modulus slightly decrease. The results show that BCHE30 is an effective β-nucleating agent for iPP.
2. The k_β values of iPP nucleated with BCHE30 first increase and then decrease until constant with the increase of BCHE30 concentration. The k_β value of iPP nucleated with BCHE30 at the concentration of 0.05 wt% reaches 87%. The results of DSC show similar tendency. The effects of the concentration of nucleating agent on the k_β values can be interpreted by the dispersibility and dual nucleating activity of BCHE30.
3. The crystallization behavior studied by DSC and POM shows that the nucleating agent BCHE30 can greatly increase the crystallization peak temperature of iPP and spherulite sizes sharply decrease with increase of the content of nucleating agent.
4. The Caze method was used to study the non-isothermal crystallization kinetics of nucleated iPP. The result indicates that the crystal growth pattern of nucleated iPP is heterogeneous nucleation followed by three-dimension spherical growth. The

crystallization active energy is determined by Kissinger method and shows that the addition of BCHE30 slightly increases the crystallization activation energy of iPP.

References

[1] Stocker W, Schumacher M, Graff S. Macromolecules 1998;31:807–14.
[2] Huo H, Jiang SC, An LJ. Macromolecules 2004;37:2478–83.
[3] Yamamoto Y, Inoue Y, Onai T. Macromolecules 2007;40:2745–50.
[4] Yoshida H. Thermochim Acta 1995;267:239–48.
[5] Padden FJ, Keith HD. J Appl Phys 1959;30:1479–84.
[6] Fujiwara Y. Colloid Polym Sci 1975;253:273–82.
[7] Lovinger AJ, Chua JO, Gryte CC. J Polym Sci Polym Phys Ed 1977;15:641–56.
[8] Leugering HJ, Kirsch G. Angew Makromol Chem 1973;33:17–23.
[9] Zhang J, Shen KZ, Na S. J Polym Sci Part B Polym Phys 2004;42:2385–90.
[10] Zheng Q, Shangguan YG, Tong LF. J Appl Polym Sci 2004;94:2187–95.
[11] Leugering HJ. Makromol Chem 1967;109:204–16.
[12] Garbarczyk J, Paukszta D. Polymer 1981;22:562–4.
[13] Garbarczyk J, Paukszta D. Colloid Polym Sci 1985;263:985–90.
[14] New Japan Chemical Co Ltd. EP 93101000.3; JP 34088/92, JP 135892/92, JP 283689/92, JP 324807/92m, (1992).
[15] Menyhard A, Varga J, Molnar G. J Therm Anal Calorim 2006;83:625–30.
[16] Feng JC, Chen MC. Polym Int 2003;52:42.
[17] Li XJ, Cheung WL. J Vinyl Addit Technol 1997;3:151–6.
[18] Varga J, Mudra I, Ehrenstein GW. J Appl Polym Sci 1999;74:2357–68.
[19] Caze C, Devaux E, Crespy A. Polymer 1997;38:497–502.
[20] Kissinger HE. J Res Natl Bur Stand (US) 1956;57:217–21.
[21] Xin Z, Zhao SC. CN 1966563A, 2006.
[22] Marco C, Gómez MA, Ellis G. J Appl Polym Sci 2002;86:531–9.
[23] Li JX, Cheung WL, Demin J. Polymer 1999;40:1219–22.
[24] Turner-Jones A, Aizlewood JM, Beckett DR. Makromol Chem 1964;75:134–59.
[25] Avrami M. J Chem Phys 1939;7:1103–12.
[26] Avrami M. J Chem Phys 1940;8:212–24.
[27] Ozawa T. Polymer 1971;12:150–8.
[28] Kim PC, Gan SN, Chee KK. Polymer 1999;40:253–9.
[29] Su ZQ, Dong M, Guo ZX, Yu J. Macromolecules 2007;40:4217–24.
[30] Varga J, Menyhárd A. Macromolecules 2007;40:2422–31.
[31] Natta G, Corradini P. Nuovo Cimento 1960;15(Suppl):40–51.
[32] Bassett DC, Block S, Piermarini GJ. J Appl Phys 1974;45:4146–50.
[33] Turner-Jones A, Cobbold AJ. J Polym Sci 1968;B6:539–46.
[34] Samuels RJ, Yee RY. J Polym Sci Part A2 1972;10:385–432.
[35] Zhang YF, Xin Z. J Appl Polym Sci 2006;101:3307–16.
[36] Jang GS, Cho WJ, Ha CS. J Polym Sci Part B Polym Phys 2001;39:1001–16.